

Analysis of Turbulent Flow over a 90° Bend of Duct Using In Centralized A. C. Plant by CFD Code

Mukesh Didwania^{1,*}, Lokesh Singh², Ashish Malik³, Mangal S Sisodiya⁴
^{1,3,4}Department of Mechanical & Automation Engineering, Amity University Rajasthan, Jaipur, India
²Department of Mechanical & Automation Engineering, Amity University Haryana, Gurgaon, India,

*Corresponding Author: mukeshdidwania4u@gmail.com

Abstract: This test case was calculated using a commercial finite volume CFD computer code ANSYS 12.0 Fluent. The geometry of Model is a three-dimensional turbulent flow over a 90° bend. Experimental setup comprising an open-circuit suction wind tunnel system for the 90° bend which is used in ducting of centralized A. C. plant in various buildings or Malls. This test case focuses on the use of approximate models such as the turbulence models to predict the physical characteristics of the turbulent flow around a 90° bend. The results from the more sophisticated Reynolds stress model are shown to better capture the anisotropy behavior of the flow in contrast to the standard k-ε model that assumes isotropy in its original model formulation and also k-w SST model use to comparison. **Finite Volume Discretization (FVM)** is employed to approximate the governing equation. Velocity and pressure distribution at bend show by simulation of fluent CFD Code. By increasing the bend length in duct, losses can be reduce.

Key words: Duct, bend, CFD, Turbulent flow, Poisson Equation, Finite Volume Discretization (FVM), interpolation scheme, standard k-ε model.

I. Introduction

CFD is the simulation of fluids engineering systems using modeling (mathematical physical problem formulation) and numerical methods (Discretization methods, Solvers, Numerical parameters, and Grid generations, etc.). Historically only Analytical Fluid Dynamics (AFD) and Experimental Fluid Dynamics (EFD) is Known. CFD made possible by the advent of digital computer and advancing with improvements of computer resources. Fluent is used to Analysis and Design Because Simulation-based design instead of “build & test” Advantages of CFD are

- (1) More cost effective and more rapid than EFD
- (2) CFD provides high-fidelity database for diagnosing flow field and also because of Simulation of physical fluid phenomena that are difficult for experiments
- (a) Full scale simulations (e.g., ships and airplanes)
- (b) Environmental effects (wind, weather, etc.)
- (c) Hazards (e.g., explosions, radiation, pollution)
- (d) Physics (e.g., planetary boundary layer, stellar evolution)
- (e) Knowledge and exploration of flow physics.

II. Experimental Setup

Experimental data are obtained on this setup using flow visualization and a Laser Doppler Anemometry (LDA) system¹. All LDA experimental measurements inside the right angled sharp 90° elbow were conducted in an open-circuit horizontal-to-vertical suction wind tunnel system located at CSIRO Process Science and Engineering. Simulation and Analysis is based on this experimental setup and detailed description of this set-up was given by Yang and Kuan (2006)¹. The 150×150 (mm²) square test section was constructed using 10mm thick Perspex, and consisted of a 3.5m-long horizontal straight duct, a right-angled sharp 90° elbow, and a 1.8m-long vertical straight duct. The geometry of the test section, the sharp 90° elbow, and the locations of LDA measurements taken are shown in Figure 1

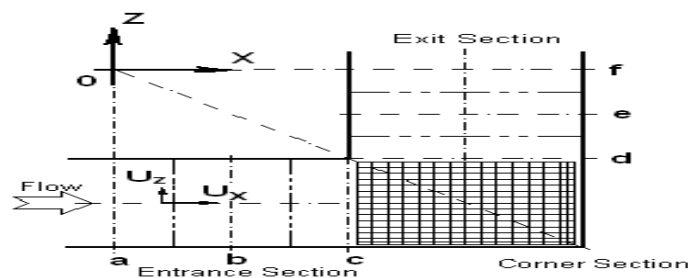


Figure 1 Schematic diagram of sharp 90° elbow section



Figure 2. Site view of Rectangular duct with 90° bends

III. Mathematical Model

Applying the fundamental laws of mechanics to a fluid gives the governing equations⁷ for a fluid. If we introduce a general variable Φ and expressing all the fluid flow equation, including equation of temperature and turbulent quantities, in the conservative incompressible form the Generic form of the Governing Equation for CFD is

$$\frac{\partial \phi}{\partial t} + \frac{\partial(u\phi)}{\partial x} + \frac{\partial(v\phi)}{\partial y} + \frac{\partial(w\phi)}{\partial z} = \frac{\partial}{\partial x} \left[\Gamma \frac{\partial \phi}{\partial x} \right] + \frac{\partial}{\partial y} \left[\Gamma \frac{\partial \phi}{\partial y} \right] + \frac{\partial}{\partial z} \left[\Gamma \frac{\partial \phi}{\partial z} \right] + S_{\phi} \quad \dots\dots\dots 1$$

Local Acceleration Term

Advection Term

Diffusion Term

Source Term

It is also called transport equation for the property Φ , it illustrates the various physical transport processes occurring in the fluid flow and this equation is usually used as the starting point for computational procedures in either the finite difference or the finite volume methods. Algebraic expression of this equation for the various transport properties are formulated and hereafter solved. By setting the transport properties Φ equal to 1, u, v, w, T, k, ϵ and selecting appropriate values for the diffusion coefficient Γ and source term S_{ϕ} , we obtain the special forms given below table for each of the partial differential equation for the conservation of mass, momentum, energy and the turbulent quantities (k- ϵ Model).

Table 1 Various transport properties, diffusion coefficients and source terms

Φ	Γ_{Φ}	S_{Φ}
1	0	0
u	$\nu + \nu_T$	$-\frac{1}{\rho} \frac{\partial p}{\partial x} + S'_u$
v	$\nu + \nu_T$	$-\frac{1}{\rho} \frac{\partial p}{\partial y} + S'_v$
w	$\nu + \nu_T$	$-\frac{1}{\rho} \frac{\partial p}{\partial z} + S'_w$
T	$\frac{\nu}{Pr} + \frac{\nu_T}{Pr_T}$	S_T
k	$\frac{\nu_T}{\sigma_k}$	$P - D$
ϵ	$\frac{\nu_T}{\sigma_{\epsilon}}$	$\frac{\epsilon}{k} (C_{\epsilon 1} P - C_{\epsilon 2} D)$

And these partial differential equations are as

Table 2 Various partial differential equations used for CFD

Mass Conservation

$$(m) \quad \frac{\partial u}{\partial x} + \frac{\partial v}{\partial y} + \frac{\partial w}{\partial z} = 0$$

Momentum Equations

$$(M_x) \quad \frac{\partial u}{\partial t} + \frac{\partial(uu)}{\partial x} + \frac{\partial(vu)}{\partial y} + \frac{\partial(wu)}{\partial z} = \frac{\partial}{\partial x} \left[(v + \nu_T) \frac{\partial u}{\partial x} \right] + \frac{\partial}{\partial y} \left[(v + \nu_T) \frac{\partial u}{\partial y} \right] + \frac{\partial}{\partial z} \left[(v + \nu_T) \frac{\partial u}{\partial z} \right] + \left(S_u = -\frac{1}{\rho} \frac{\partial p}{\partial x} + S'_u \right)$$

$$(M_y) \quad \frac{\partial v}{\partial t} + \frac{\partial(vv)}{\partial x} + \frac{\partial(vv)}{\partial y} + \frac{\partial(wv)}{\partial z} = \frac{\partial}{\partial x} \left[(v + \nu_T) \frac{\partial v}{\partial x} \right] + \frac{\partial}{\partial y} \left[(v + \nu_T) \frac{\partial v}{\partial y} \right] + \frac{\partial}{\partial z} \left[(v + \nu_T) \frac{\partial v}{\partial z} \right] + \left(S_v = -\frac{1}{\rho} \frac{\partial p}{\partial y} + S'_v \right)$$

$$(M_z) \quad \frac{\partial w}{\partial t} + \frac{\partial(wv)}{\partial x} + \frac{\partial(vw)}{\partial y} + \frac{\partial(wv)}{\partial z} = \frac{\partial}{\partial x} \left[(v + \nu_T) \frac{\partial w}{\partial x} \right] + \frac{\partial}{\partial y} \left[(v + \nu_T) \frac{\partial w}{\partial y} \right] + \frac{\partial}{\partial z} \left[(v + \nu_T) \frac{\partial w}{\partial z} \right] + \left(S_w = -\frac{1}{\rho} \frac{\partial p}{\partial z} + S'_w \right)$$

Energy Equation

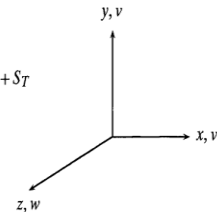
$$(E) \quad \frac{\partial T}{\partial t} + \frac{\partial(uT)}{\partial x} + \frac{\partial(vT)}{\partial y} + \frac{\partial(wT)}{\partial z} = \frac{\partial}{\partial x} \left[\left(\frac{\nu}{Pr} + \frac{\nu_T}{Pr_T} \right) \frac{\partial T}{\partial x} \right] + \frac{\partial}{\partial y} \left[\left(\frac{\nu}{Pr} + \frac{\nu_T}{Pr_T} \right) \frac{\partial T}{\partial y} \right] + \frac{\partial}{\partial z} \left[\left(\frac{\nu}{Pr} + \frac{\nu_T}{Pr_T} \right) \frac{\partial T}{\partial z} \right] + S_T$$

Turbulence Equations

$$(k) \quad \frac{\partial k}{\partial t} + \frac{\partial(uk)}{\partial x} + \frac{\partial(vk)}{\partial y} + \frac{\partial(wk)}{\partial z} = \frac{\partial}{\partial x} \left[\frac{\nu_T}{\sigma_k} \frac{\partial k}{\partial x} \right] + \frac{\partial}{\partial y} \left[\frac{\nu_T}{\sigma_k} \frac{\partial k}{\partial y} \right] + \frac{\partial}{\partial z} \left[\frac{\nu_T}{\sigma_k} \frac{\partial k}{\partial z} \right] + (S_k = P - D)$$

$$(ε) \quad \frac{\partial ε}{\partial t} + \frac{\partial(uε)}{\partial x} + \frac{\partial(vε)}{\partial y} + \frac{\partial(wε)}{\partial z} = \frac{\partial}{\partial x} \left[\frac{\nu_T}{\sigma_ε} \frac{\partial ε}{\partial x} \right] + \frac{\partial}{\partial y} \left[\frac{\nu_T}{\sigma_ε} \frac{\partial ε}{\partial y} \right] + \frac{\partial}{\partial z} \left[\frac{\nu_T}{\sigma_ε} \frac{\partial ε}{\partial z} \right] + \left(S_ε = \frac{ε}{k} (C_{ε1}P - C_{ε2}D) \right)$$

$$\text{where } P = 2\nu_T \left[\left(\frac{\partial u}{\partial x} \right)^2 + \left(\frac{\partial v}{\partial y} \right)^2 + \left(\frac{\partial w}{\partial z} \right)^2 \right] + \nu_T \left[\left(\frac{\partial u}{\partial y} + \frac{\partial v}{\partial x} \right)^2 + \left(\frac{\partial v}{\partial z} + \frac{\partial w}{\partial y} \right)^2 + \left(\frac{\partial w}{\partial x} + \frac{\partial u}{\partial z} \right)^2 \right] \text{ and } D = ε$$



These equations form a set of coupled, nonlinear partial differential equations. It is not possible to solve these equations analytically for most engineering problems.

However, it is possible to obtain approximate computer-based solutions to the governing equations for a variety of engineering problems. This is the subject matter of Computational Fluid Dynamics (CFD).

The governing equations are non-linear partial differential equations for which a closed form solution is not possible. The computational fluid dynamics software "Fluent", which uses a control volume-based finite difference method, was chosen to solve these equations, due to its general capability, user-friendliness, and availability to the author.

Three turbulent models were used in this work to examine which one predicts the flow most closely to the values measured at the advanced Laser Diagnostic Laboratory at CSIRO. These turbulent models are the k-ε realizable (Shih et al, 1995), the k-ε RNG (Yakhot & Orszag, 1986 and Choudhury, 1993), and the Reynolds stress model (Speziale et al, 1991).

IV. Model Description

The geometry of Model is a three-dimensional turbulent flow over a 90° bend. Experimental setup comprising an open-circuit suction wind tunnel system for the 90° bend. Which comprises of a 3.5 m-long horizontal duct, a 90° bend with a 150 x 150 mm² square test section, and a 2 m long vertical straight duct. Air flows through a 10 mm thick Perspex square test section with the bulk gas velocity U_b adjusted through the aid of a variable frequency controller.

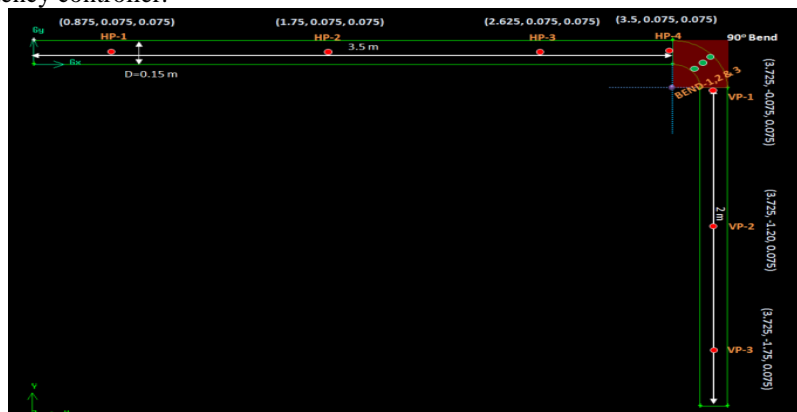


Figure 3. -Computational Domain of Rectangular Duct of bent as Bend radius = Depth of Duct

V. Grid Generation

Grid generation for the 90° square section bend, the computational domain begins at a distance of 2D upstream from the bend entrance and extends to 20D downstream from the bend exit. Poisson Equation for the pressure correction that is solved through the default iterative solver, normally the multigrid solver in the ANSYS Inc., Fluent computer code Prior to the CFD Simulation, computational meshes were generated for each point of duct and Hexagonal submap type mesh is generated using GAMBIT tool in Fluent.

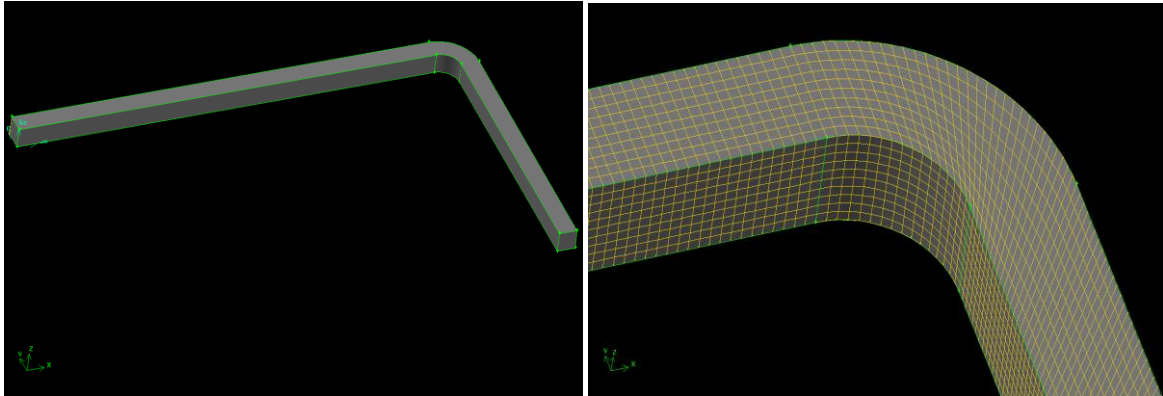


Figure 4.- Model view of Duct & Hexagonal type Mesh of Duct of 39700 cells.

Table 3 Mesh description

File Name	Mesh Type	Total Mesh in Domain	Spacing
90 bend (2-D).dbs	Quad Sub Map	3658	0.015
90 bend in 3-D.dbs	Hex Submap	8604	0.025
90 bend in 3-D(B).dbs	Hex Submap	39700	0.015
90 bend in 3-D(C).dbs	Hex Submap	134325	0.01

VI. Boundary Conditions

Boundary condition at the inlet, Dirichlet conditions are used for all variables. At the outlet, Neumann boundary conditions are applied for all the transported variables

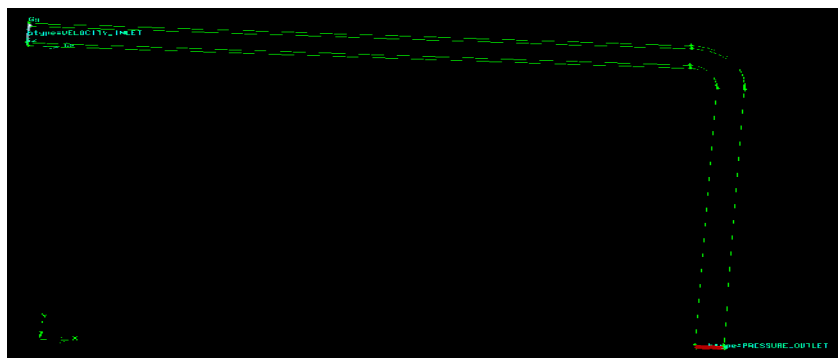


Figure 5- Boundary conditions for Duct

At inlet, velocity is define and the inlet air temperature will set to 280 K. The inlet velocity depends on the chosen Reynolds number.

At outlet, pressure is putting for simulation.

The side walls were modeled to be adiabatic with zero heat flux. The no slip condition was applied and zero velocity in the tree direction ($U_x=U_y=U_z=0$) was used.

VII. CFD Simulations

Three dimensional Unsteady CFD Analysis Was performed for solving the momentum, continuity and energy equations. The modified k-e turbulence model was used to describe turbulence transport, with the both standard wall function model for near wall treatment. Finite Volume Discretization (FVM) is employed to approximate the governing equation. Interpolation scheme is employed for solution of governing equation

VIII. Features of The Simulation

- This study illustrates the importance of evaluating the choice of the turbulence models for computing the flow separation around the 90° bend.
- Working fluid is considered to be incompressible.
- Default initial conditions implemented in the computer code are used for the simulations.
- Reduction of pressure at bend section.

IX. Result And Discussions

Pressure distribution in Duct

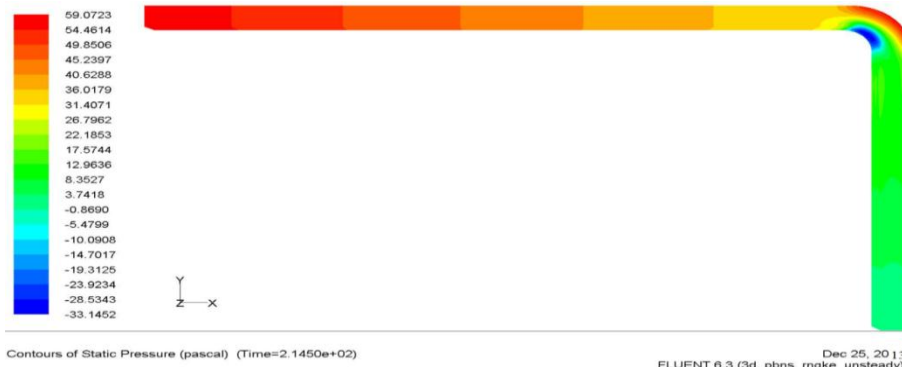


Figure 6.- Pressure distribution in Duct

Comparison of pressure difference at Bend

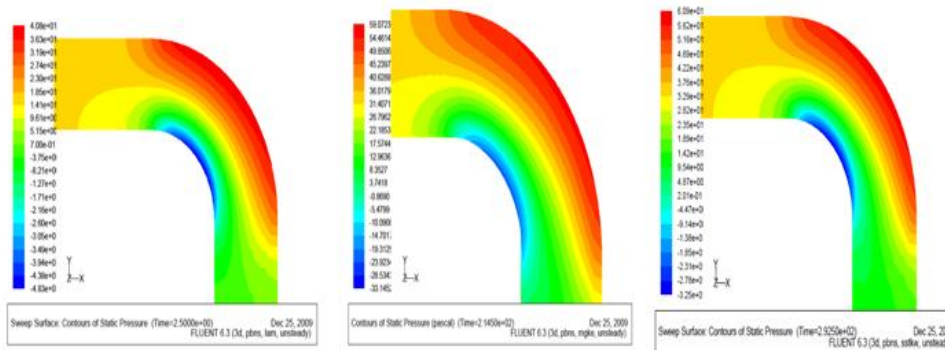


Figure 7.-Laminar flow

Figure 8.Turbulent Flow (k-w SST& K-ε RNG model)

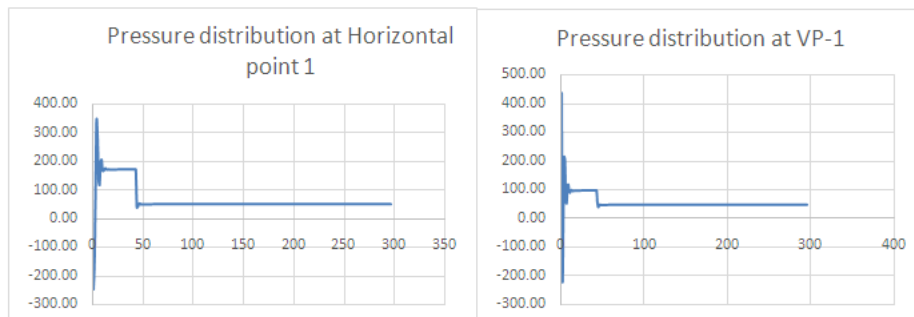


Figure 9. XY Chart of pressure distribution in Duct at various points

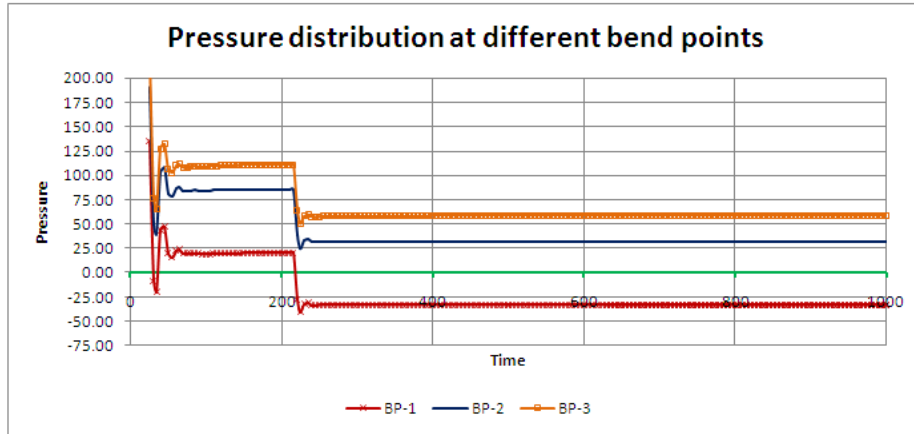


Figure 10. XY Chart of pressure distribution in Duct at various bend points

Comparison of Velocity distribution

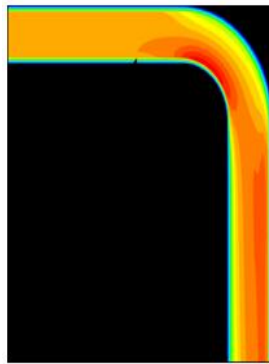


Figure 11. -Laminar flow

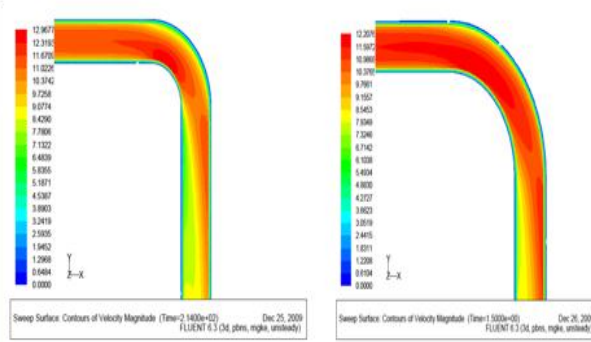


Figure 12. -Turbulent flow (K-ε RNG model& k-w SST)

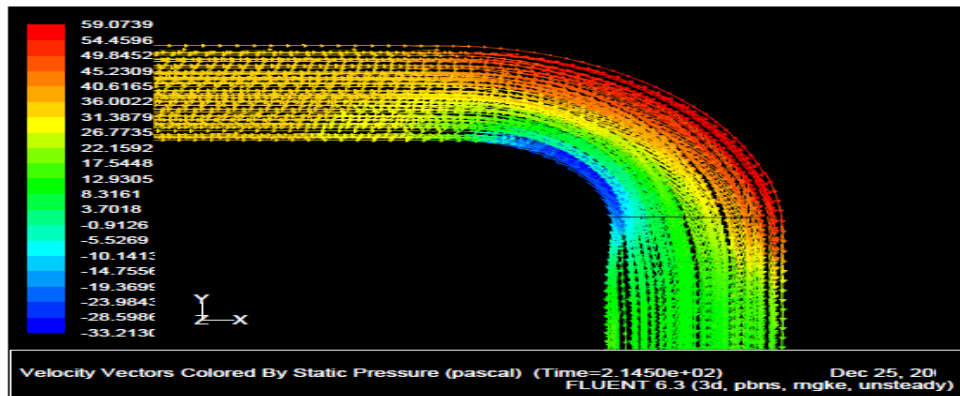


Figure13: Velocity vector of turbulent flow (k-ε RNG model)

In this study we can say

- K-ε RNG model is better than other models
- Validation with experimental results is must so that selection of turbulence model is justified.
- In whole part of duct velocity distribution is uniformed but at bend it is not true.
- We can see in figure 6, Pressure is high at inlet and gradually decreases in the duct but suddenly increases at bend section.
- So Bend size play important role in case of pressure distribution

X. Comparison of Pressure of Different Sizes of Bend (K ε- RNG Model)



Figure 14. Duct using Different bend sizes

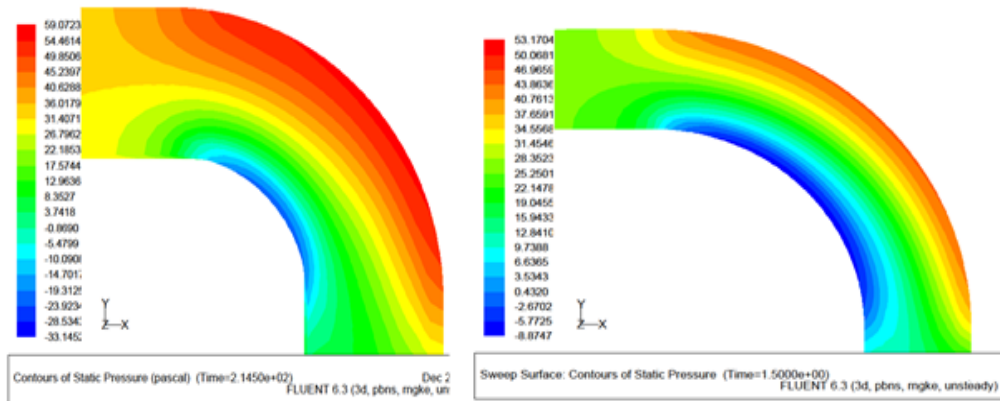


Figure 15. – Simulation of Flow in Duct using Different bend sizes

XI. Conclusion

- In this study we focus on the use of approximate models such as the turbulence models to predict the physical characteristics of the turbulent flow around a 90° bend.
- The flow around a 90° bend though geometrically simple exhibits complex flow structures due to the existence of secondary flows in the vicinity of the bend region, which are generally anisotropic in nature.
- We can see in figure 6, Pressure is high at inlet and gradually decreases in the duct but suddenly increases at bend section so we can conclude that if we use large bend size (large radius of bend section) it will reduce pressure at bend section (figure 10) and further reduce losses at bend section.

XII. Future Scope

We can analysis on these points in future

- (1) Pressure drop increases with airflow (CFM) increases.
- (2) Pressure variation if pipe Length increases but airflow stays the same.
- (3) Analysis of flow through convergent -Divergent Duct.
- (4) Analysis of heat transfer through cold fluid flowing in the Duct.

References

- [1]. YANG, W. and KUAN, B., (2006), "Experimental investigation of dilute turbulent particulate flow inside a curved 90° bend", *Chemical Engineering Science*, **61**, 3593–3601.
- [2]. KUAN, B., YANG, W. and SCHWARZ, M.P., (2007), "Dilute gas-solid two-phase flows in a curved 90o duct bend: CFD simulation with experimental validation", *Chemical Engineering Science*, **62**, 2068–2088.
- [3]. SHIH, T.-H., LIOU, W.W. SHABBIR, A., YANG, Z. and ZHU, J., (1995), "A new k-ε eddy-viscosity model for high Reynolds number turbulent flows – Model development and validation", *Computers Fluids*, **24(3)**, 227–238.
- [4]. YAKHOT, V. and ORSZAG, S.A., (1986), "Renormalization group analysis of turbulence: I. Basic theory", *J. Scientific Computing*, **1(1)**, 1–51.
- [5]. Icoz, T., and jaluria, Y., 2005. Numerical Simulation of boundary conditions and the Onset of Instability due to the protruding thermal Sources in an Open Rectangular channel, *Numerical Heat Transfer, part A*, **48**, 831-847.
- [6]. P. mallikarjuna Reddy, K. Rajagopal and k. Govindarajulu, deptt of Mechanical engg , G. Pulla Ready Engg college Kurnool 518002, Andhra Pradesh, India, Simulation of Heat Transfer in S.I. engine Combustion Chamber.
- [7]. JiyuanTu, Guan Heng, Liu, RMIT University, Australia, Computational Fluid Dynamics, A practical Approach, ELSEVIER B H, CFD Simulation Analysis-Essentials.
- [8]. N.C. Markatos, K.A. Pericleous, Laminar and turbulent natural convection in an enclosed cavity , *Int. J. Heat Mass Trans.* 27 (5) (1984) 755±772
- [9]. Karwa R, Solanki SC, Saini JS. Heat transfer coefficient and friction factor correlations for the transitional flow regime in rib roughened rectangular ducts. *International Journal of Heat and Mass Transfer* 1999; 42:1597–615.
- [10]. S. C. Arora, S. Domkundwar, A course in Refrigeration and Air Conditioning Dhanpatrai& Co. delhi., 2007, chapter- 23 (23.1-23.40).